Revista Brasileira de Geografia Física v.17, n.05 (2024) 3620-3641.

Revista Brasileira de Geografia Física

ISSN:1984-2295

Homepage: https://periodicos.ufpe.br/revistas/rbgfe

The Application of Remote Sensing and Geoprocessing in Coastal Geomorphological Characterization: A Case Study in Paranaguá and Superagüi Strandplains, Southern Brazil[1]

Shaiely F. dos Santos[1], Maria C. de Souza[2], Rodolfo J. Angulo[3], Marcelo Bogo[4], Maria Luiza C. C. Rosa[5]

[a]Ph.D. in Geology, Coastal Studies Laboratory, Department of Geology at the Federal University of Paraná (UFPR), Av. Cel. Francisco H. dos Santos, 210, Jardim das Américas, Curitiba/PR, fer.shay@gmail.com (https://orcid.org/0000-0002-2534-4702); Corresponding author: fer.shay@gmail.com. [b]PhD in Geology, Full Professor of the Geology Department, Graduate Program in Geology and Coastal Studies Laboratory coordinator at the Federal University of Paraná (UFPR), Av. Cel. Francisco H. dos Santos, 210, Jardim das Américas, Curitiba/PR, cristinasouza2527@gmail.com (https://orcid.org/0000-0002-8702-7550). [c]PhD in Geosciences, Senior Professor of the Graduate Program in Geology and Coastal Studies Laboratory coordinator at the Federal University of Paraná (UFPR), Av. Cel. Francisco H. dos Santos, 210, Jardim das Américas, Curitiba/PR, fitoangulo@gmail.com (https://orcid.org/0000-0001-9261-3004). [d]PhD in Geology, Professor of the Geology Department at the Federal University of Santa Catarina, R. Eng. Agronômico Andrei Cristian Ferreira, 240-432 - Carvoeira, Florianópolis/SC, bogo.marcelo@gmail.com (https://orcid.org/0000-0002-8844-951X). [e] PhD in Geology, Full Professor of the Geodesy Department and Graduate Program in Geosciences at the Federal University of Rio Grande do Sul (UFRGS), Paulo Gama, 110, Anexo I da Reitoria - Prédio 12106 - Porto Alegre/RS, luiza.camara@ufrgs.br (https://orcid.org/0000-0002-1963-4842)

Artigo recebido em 04/01/2024 e aceito em 02/06/2024

A B S T R A C T

This paper presents the combination of remote sensing and geoprocessing to create geomorphological maps of the Paranaguá and Superagüi strandplains, a coastal region in southern Brazil, South America. Optical images and Geographic Information System tools provide a broad view of different geomorphological aspects existing in a location, which helps in the analysis and understanding of the geological evolution of an area. Therefore, digital processing of images from the Landsat 8 OLI datasets, and relief analysis with the Digital Surface Model of the Shuttle Radar Topography Mission was carried out, also integrating with optical images extracted from Google Earth™ and previous geological map. The geomorphological characterization carried out by visual interpretation resulted in the separation of seven main classes, designated as 1) crystalline basement; 2) internal marine terrace; 3) external marine terrace; 4) beach ridge; 5) beach; 6) paleoestuarine plain; and 7) tidal flat/mangrove. In general, the combined utilization of remote sensing products yielded satisfactory results in distinguishing these categories, while the relief analysis confirmed their delineation. Integrating remote sensing methodologies with geoprocessing emerges as an indispensable asset in coastal evolution research, particularly due to the presence of diverse depositional environments that yield distinct features, and the ever-evolving nature of this region.

Keywords: Optical image analysis, Landsat 8 OLI, SRTM, Coastal evolution

Aplicação do sensoriamento remoto e geoprocessamento na caracterização geomorfológica costeira: um estudo de caso nas planícies de Paranaguá e Superagüi, sul do Brasil

R E S U M O

Este artigo apresenta a combinação de sensoriamento remoto e geoprocessamento para criar mapas geomorfológicos das planícies costeiras de Paranaguá e Superagüi, região costeira no sul do Brasil, América do Sul. As imagens ópticas e as ferramentas do Sistema de Informação Geográfica proporcionam uma visão ampla dos diferentes aspectos geomorfológicos existentes em um local, o que auxilia na análise e compreensão da evolução geológica de uma área. Portanto, foi realizado o processamento digital das imagens dos conjuntos de dados do Landsat 8 OLI e a análise do relevo com o Modelo Digital de Superfície da Shuttle Radar Topography Mission - SRTM, integrando também com imagens ópticas extraídas do Google Earth™ e mapa geológico. A caracterização geomorfológica realizada por interpretação visual resultou na separação de sete classes principais, designadas como 1) embasamento cristalino; 2) terraço marinho

[1] Trabalho extraído da tese de doutoramento intitulada "Arquitetura deposicional e cronologia das barreiras pleistocênicas paranaenses", orientada pela prof.ª Maria C. de Souza na Universidade Federal do Paraná.

interno; 3) terraço marinho externo; 4) cordões litorâneos; 5) praia; 6) planície paleoestuarina; e 7) planície de maré/manguezal. Em geral, a utilização combinada de produtos de sensoriamento remoto produziu resultados satisfatórios na distinção destas categorias, enquanto a análise do relevo confirmou a sua delimitação. A integração de metodologias de sensoriamento remoto com geoprocessamento surge como um trunfo indispensável na investigação da evolução costeira, particularmente devido à presença de diversos ambientes deposicionais que produzem características distintas, e à natureza em constante evolução desta região.
Palavras-chave: Análise de imagem óptica, Landsat 8 OLI, SRTM, Evolução costeira.

Introduction

The coastal region is characterized by numerous interactions involving physical factors from land, sea, and atmosphere. In a transition zone between the continent and the ocean, this complex dynamic results in continuous changes in this area's morphology, vegetation, and sedimentary composition. Changes occur due to oceanic processes, such as waves, tides, and currents, as well as continental factors, such as river discharge and ice melt, and climatic and meteorological conditions, including precipitation and winds, and all the dynamics of sediment transport influenced by fluids, geology, and topography. Changes are also caused by human influences, such as the degradation of ecosystems (Cowell and Thom, 1994; Silva et al., 2004). Geomorphological mapping in the coastal zone represents the characteristics of the relief and its constant transformations that act on the region, whether from natural or anthropogenic processes (Rodrigues et al., 2023).

The geoprocessing of remote sensing data makes it possible to map, measure and analyze several geomorphological aspects that assist in understanding the geological evolution of a coastal region (e.g., Butler and Walsh, 1998; Rosa et al., 2007; Wu, 2007; Kawakubo, 2011; Polizel and Rossetti, 2014; Leal and Barboza, 2016; Radaideh et al., 2016; Sarmiento et al., 2016; Bishop-Taylor et al., 2021; Hansen et al., 2021; Mao et al., 2022; Wang et al., 2022).

In Parana State, southern Brazil, even with the densely forested area on the coastal zone, satellite images show the morphological features very well, especially in outer parts of the plain, such as the beach ridges, which is one of the most striking characteristics of the region (Angulo, 1992), represented by a shore-parallel and subparallel, narrow, elongated sand ridge (NNE/SSW). These beach ridges, as well as eolian dunes, make up coastal barriers (Otvos, 2012), formed in relative sea level variation (RSL), in agreement with other allogenic factors, such as climate tectonics, and autogenic factors, related to coastal dynamics (Davis Jr. and FitzGerald, 2004; Otvos, 2020).

The region is covered by two main geological domains: the domain of rocks of the Paraná shield/basement formed by igneous and metamorphic rocks, with ages varying from the Archean to the Proterozoic, and the domain of the Cenozoic sedimentary cover formed by unconsolidated sediments, of continental and marine (Martin et al., 1988; Angulo, 1992). The study area, coastal plain, is located within the Cenozoic sedimentary cover, dating from the Quaternary period.

According to Guedes et al. (2020), the Paraná coastal plain is constituted by at least three barrier systems corresponding to transgressive-regressive events. One of Middle Pleistocene age (~195 to 220 ky) was discovered by them, and two others of Upper Pleistocene age (~120 to 125 ky) and Holocene age (~6 to 0 ky), described by Martin et al. (1988), Angulo and Suguio (1995), Lessa et al. (2000), which can be correlated to Marine Isotope Stages (MIS) 7e, 5e and 1, respectively (Rosa, 2012; Lopes et al., 2014; Guedes et al., 2020). In the Rio Grande do Sul State, these systems correspond to high-frequency depositional sequences, called Systems I, II, III, and IV (Villwock et al., 1986; Rosa et al., 2017). The boundary between the barrier generations has been presented by Souza (2012), Angulo et al. (2008), Guedes et al., (2020), Bogo et al., (2021), and Bogo et al., (2023), through geological and geomorphological mapping, morphostratigraphy, drilling, geochronology, and geophysical surveys.

Thus, analyzing coastal barriers is a fundamental part of studying the formation and evolution of coastal plains in Brazil, since the country has an extensive coastal zone with areas of great economic development and population concentration.

According to estimates by the Brazilian Institute of Geography and Statistics - IBGE (2022), 301,405 inhabitants live on the coast of Paraná and depend directly and indirectly on the coastal region to survive. In Paranaguá Bay, a large port activity is concentrated due to the Dom Pedro II port through the export of soybeans, vegetable oil, sugar, corn, paper, wood, vehicles, fertilizers, among others.

Understanding the formation and evolution of environments that make up the coast helps human activities, for instance in the growing urbanization and the tourist sector, and knowledge about the present depositional systems since they are short- to long-term natural processes (Mumby and Edwards, 2000; Lu et al., 2022; Benavente et al., 2023; Munasinghe and Warnasuriya, 2023; Singh et al., 2023, Biswas et al., 2024).

According to Walsh et al. (1998), geoprocessing of remote data techniques allows the evaluation of the space-time variability of an area, the geological structures, the set of landscape perspectives, and the biophysical processes.

It is understood that the production of geomorphological maps is essential for understanding the Earth's surface and the processes that shape it, also the maps serve as an indispensable instrument for a multitude of purposes, including urban and environmental planning, resource management, volcanic eruptions, and floods, and to create strategies for management and mitigation of natural disasters (e.g Griffiths and Abraham, 2008; Zangana, 2023).

Geomorphological mapping has gained increasing importance in recent years. A variety of techniques have been developed and applied to produce more accurate and update mapping, including remote sensing and other available geotechnologies, as shown by Sánchez et al., (2021), Vargas et al., (2021), Giaccone et al., (2022); Quesada-Román and Peralta-Reys, (2023), Zhang et al., (2023), Chen et al., (2024) and Yu et al., (2024).

Therefore, the primary objective of this study is to undertake a geomorphological characterization of the Paranaguá and Superagui strandplains with different depositional environments through digital image processing, renewing and improving maps that characterize the coastal region. This aims to delineate distinct morphological units and their associated characteristics along the Paraná coastline by combining various data products. Also, use different combinations of spectral bands to define which better represent the mapped units and coastal features.

Geoprocessing tools were employed to achieve this, including analyzing optical imagery from Landsat 8 OLI, from the National Institute for Space Research (INPE) website, and a digital surface elevation model (DSM), from Shuttle Radar Topography Mission (SRTM). For creating the maps and processing the satellite images, the free software QGIS® 3.16 was utilized.

Additionally, the study was assisted by the insights the geological map and Google Earth imagery provided to enhance detailed analysis, highlighting the benefit of integrating data and methods for research results.

Materials and methods

Study area

The Paranaguá and Superagüi strandplains, in southern Brazil, are formed mainly by barrier sedimentary deposits developed during periods of higher relative sea level than present in the Quaternary (Figure 1). Three events were recorded on the coast, referring to the Middle and Upper Pleistocene (barriers II and III) and the Holocene (barrier IV) (Angulo, 1992; Lessa et al., 2000; Guedes et al., 2020), corresponding to Lagoon-Barrier II, III, and IV Systems, documented in the Rio Grande do Sul State, as presented by Villwock and Tomazelli (1995), Tomazelli and Villwock (2000), Tomazelli and Villwock (2005), Rosa (2012) and Rosa et al. (2017). In general, these barriers are composed of fine to very fine sand, with a subordinate content of coarse sand and gravel (Angulo, 1993; Souza, 2012).

The landscape is further characterized by the distinctive formation of prograded beach ridges, and elongated sand ridges that run parallel to the shoreline (Otvos, 2000), resembling a topographical feature referred to as a strandplain. Alongside the prominence of coastal ridges, the coastal region is also recognized for hosting estuarine complexes rich in mangrove ecosystems and deposits from ancient estuarine, as emphasized by Angulo et al. (2009). Further insights into the formation and evolution of the Paraná coastal plain region are provided by a series of studies. Noteworthy contributions come from Bigarella (1946, 1971), Angulo (2004), as well as Angulo et al. (2002, 2008). Additionally, the work of Machado and Pinto (2017) and Guedes et al. (2020) offers valuable perspectives on this subject.

Methodologies

To execute this work, the following methodologies were applied: digital processing of optical images, a digital surface model (DSM), and the creation of a geomorphological map. The selected satellite images were Landsat 8 OLI datasets with 30 m spatial resolution (15 m in the panchromatic band), and a radiometric resolution of 16 bits per pixel, registered in July 2020 and sourced free from the National Institute for Space Research (INPE) website. The acquisition of the Digital Surface Model (DSM) was facilitated through the Shuttle Radar Topography Mission (SRTM), a dataset made accessible by the United States Geological Survey (USGS), and subsequently enhanced by Topodata to achieve a vertical resolution of 30 m (available at www.dsr.inpe.br/topodata). For the maps elaboration and the satellite image processing, the free software QGIS®3.16 was used.

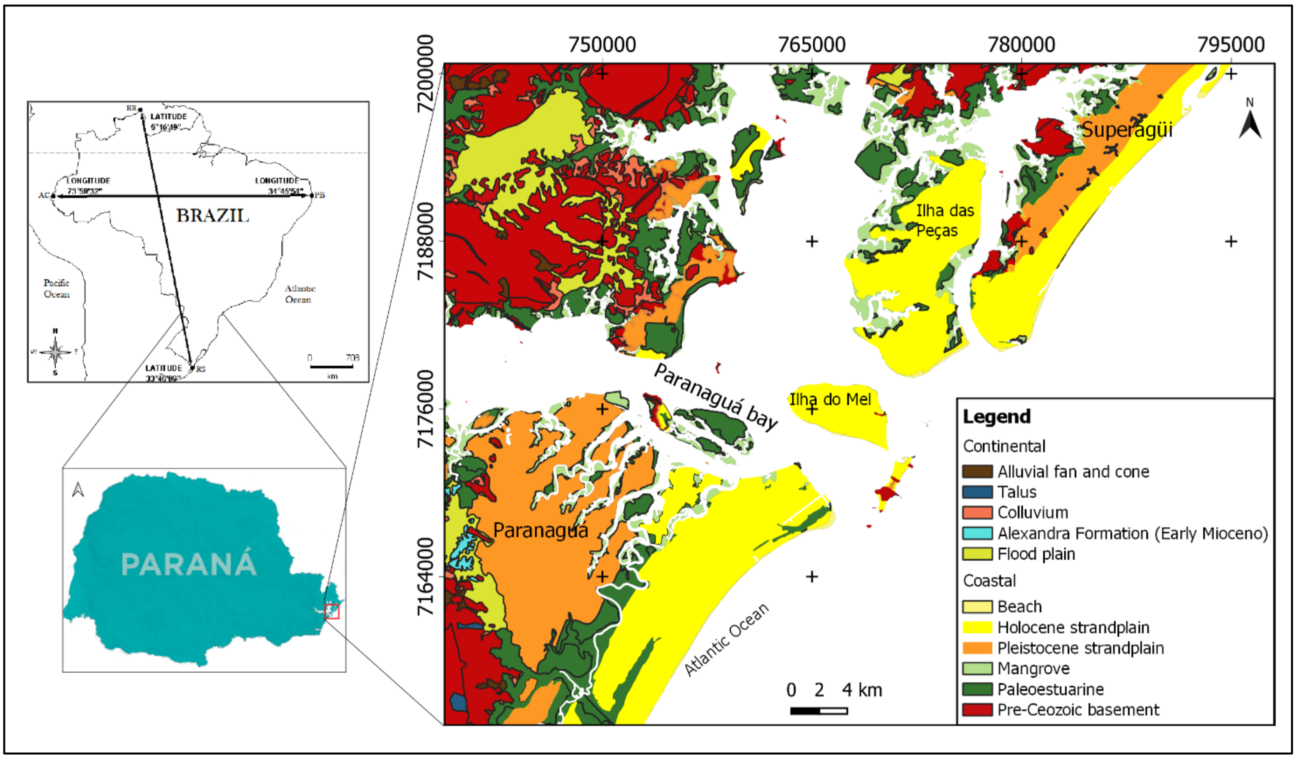

Figure 1. Geological map of the study area (based on Angulo, 2004).

Optical image digital processing

To enhance the visibility of geological structures and landforms, the satellite images underwent a pre-processing routine in the software encompassing: 1) atmospheric correction, this correction aimed to mitigate the impact of molecular dispersion, aerosols, and absorption by gases like oxygen, ozone, and water vapor (Liang et al., 2001). The correction can be performed simultaneously for all bands when inserting them into the software, in the option SPC > Preprocessing tool > Landsat; 2) georeferencing in UTM projection, DATUM - SIRGAS 2000, Zone 22S, in Raster > Projections > Reproject Coordinates; 3) study area clipping; and 4) spectral analysis of curves in the histogram as a linear contrast enhancement technique to improve the visual quality of images, for instance, a variation in image contrast allows the frequency histogram related to the gray levels present in the image to be expanded, leading to a greater distribution in the tones present in the scene to assist in the characterization of geomorphological features.

Following this, the digital processing technique of image color composition was employed, rendering the imagery more discernible and human-eye sensitive compared to monochromatic representations, select Raster > Miscellanea > Merge > Input layer (select bands) > Each input file in a separate band > Execute > Layer properties > Symbology. Multiple color composites were generated to accentuate distinct environments crucial for the geomorphology map's composition. Distinct wavelengths frequently offer enhanced discriminatory capabilities for specific features. As an example, the Near Infrared (NIR) wavelength is frequently employed in multispectral sensors due to the pronounced reflectance of vegetation in this segment of the electromagnetic spectrum. This spectral information proves highly valuable when conducting vegetation analyses. The Shortwave Infrared (SWIR) bands featured on Landsat 8 instruments are highly effective in discriminating disparities in exposed terrain and in distinguishing between wet and dry conditions within a given scene (Peters, 2015).

According to Jensen (2009) and Meneses and Almeida (2012), when identifying elements and interpreting satellite images, it is common to use primary elements such as tone and color, and secondary elements such as size, shape, and texture. Florenzano (2007), refers to the texture as having a smooth, uniform, or rough appearance, and the colors can be differentiated in variations of scenes and with darker and/or lighter tones. Primary factors in the interpretation of this work included color, texture, and relief forms. The classes and band compositions used for the geomorphological mapping are presented in Table 1. Optical image analysis was complemented with high-resolution data from Google Earth™.

Digital surface model

To extract intricate morphological details, accentuate coastal characteristics, and refine the delineation of subunits, maps were synthesized utilizing SRTM data as a valuable tool in facilitating the creation of the ultimate map rendition, in Adding Raster Layer tool. From this, altitude (digital surface model), slope, aspect, and RGB composite maps were created. For the altitude map, the variables were selected in Layer properties > Symbology, a linear interpolator was selected with a color palette with 20 classes ranging from 0 to 50 meters. For create slope map, selected Raster > Analysis > Slope, after running the map, select Layer properties > Symbology, 7 classes were defined, ranging from 0 to 10 degrees, and a linear interpolator. To create the aspect map, select Raster > Analysis > Aspect. The discrete method interpolator was used for the aspect map divided the 360 degrees into N, NE, E, SE, S, SW, W, and NW directions. Starting with 22.5 degrees = N, 67.5 = NE, 112.5 degrees = E, 157.5 degrees = SE, 202.5 degrees = S, 247.5 degrees = SW, 292.5 degrees = W, and 337.5 degrees = NW, these variables are organized under Layer Properties > Symbology.

The RGB composite is a map resulting from the integration of altitude (R), slope (G), and aspect (B) data. Processed analogously to color compositions of optical images, one of the primary colors is assigned to each variable. Hence, red predominates in higher areas, green stands out in steeper slopes, and regions with higher azimuths feature the color blue. Additionally, a topographic profile perpendicular to the current coastline was traced on each strandplain over the MDS indicating the geomorphological units/subunits mapped.

Geomorphological map creation

The amalgamation of visual interpretation derived from Landsat 8 optical imagery, data from the digital surface model, field analysis, Google Earth imagery, and geological mapping, the process facilitated the distinct identification and subsequent mapping of various geomorphological units. These units were delineated and charted using the QGIS® 3.16 software platform. The map was based on the relief taxonomy used by IBGE (2009) present in the geomorphology technician's manual. As a guide for the interpretation, the third taxonomic level was used, which corresponds to geomorphological units, and the fourth level, which relates the geomorphological subunits referring to accumulation models. Elaborations regarding the colors and textures characteristic of the coastal environments, as discerned from the images, have been expounded upon in Table 1.

Table 1 - Elements and classes interpreted for the elaboration of the geomorphological map.

Classes \ characteristics	Morphology/localization	Band composition	Tonality and color	Texture
Crystalline basement (BA)	High relief in the inner plain	432 	Green tonality with shaded features	Rougher texture
Internal marine terrace (IMT)	Inner plain with gently undulating relief	432 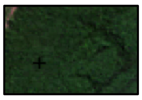	Dark green and low reflectance	Dense vegetation with a rough texture
External marine terrace (EMT)	Between the inner plain and the ocean, flat terrain with beach ridges presence	652 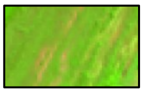	Green vegetation and light brown exposed soil	Smooth and rough
Beach ridge (BR)	Linear features, shore-parallel, and sub-parallel	543 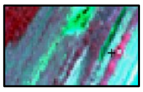	Ridges in red tonality and dark color between them	Smooth and rough
Beach (BE)	Linear strip on the coast	765 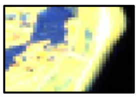	White and yellow with high reflectance	Smooth texture
Paleoestuarine plain (PP)	Between the two terraces, in the inner plain, headwaters of a drowned drainage system	543 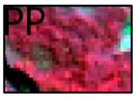	Dark shade of red	Rougher texture
Tidal flat/mangrove (MA)	Bordering the interior of the plains with low-altitude	562 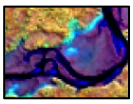	Brown tonality and low reflectance	Smooth texture

Results and discussion

Optical Image Analysis

Two distinct geomorphological units were discerned: the crystalline basement and the coastal plain. Further subdivision of the plain led to the recognition of six individual subunits, categorized following the 4th taxonomic level as outlined by the accumulation models proposed by IBGE in 2009. These subunits encompassed the internal marine terrace, external marine terrace, paleoestuarine plain, tidal flat/mangrove, beach, and beach ridges shown in Figures 11, 12, and Table 1.

Crystalline basement (BA)

The crystalline basement is the highest unit in the coastal zone, present in the Serras region (IPARDES, 1990) formed by igneous and metamorphic rocks from the Pre-Cenozoic, originated by dissection of the plateau edge (Angulo, 1992; 2004). Characterized by undulating topography marked by ridges, this formation possesses the steepest slopes within the coastal region (Figure 2). Although this unit is discernible across all color composites, the decision was made to employ the true color composite R4/G3/B2 to clearly illustrate its demarcation.

The present vegetation presents reflectance in band 3 (G-green) with low reflectance in the shaded area of the hill. The bare soil stands out in stark contrast to the surrounding vegetation, as depicted by band 4 (R – red), while the water bodies manifest as distinct blue tones through band 2 (B – blue). The utilization of the MDS also played a pivotal role in outlining the basement unit, primarily due to the significant disparity in elevation between this particular unit and the coastal plain, with the former boasting an altitude exceeding 50 meters (Figures 9 and 10).

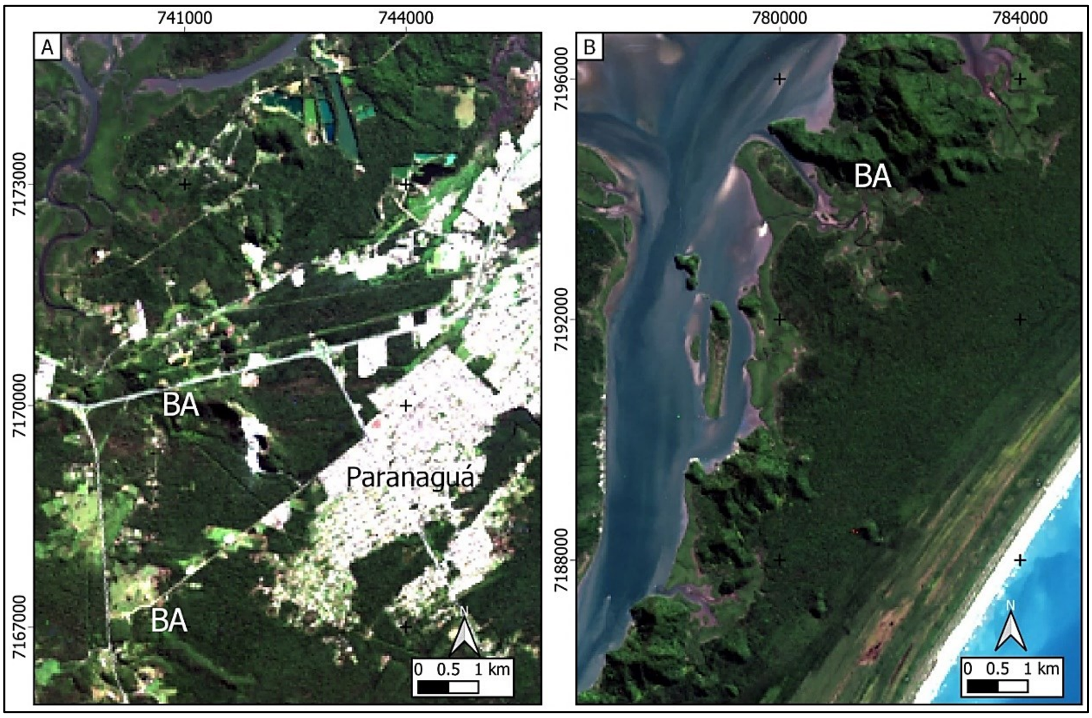

Figure 2. Crystalline basement (BA) showed by Landsat 8 true color composition R4/G3/B2 with linear contrast enhancement: A) Paranaguá strandplain and B) Superagüi strandplain.

Internal marine terrace (IMT)

Located in the inner portion of the coastal plain, the internal marine terraces are of Pleistocene age (Angulo, 1992; Lessa et al., 2000; Guedes et al., 2020) formed during transgressive-regressive events 220 ky and 120 ky ago, when the sea level reached 10 m and 8 m above current sea level. The terrace is cut by numerous river channels and marked by the headwaters of a drowned drainage system that ends abruptly in contact with the younger terrace (Figure 3). The city of Paranaguá is situated on this particular terrace, identifiable in Figure 3 by its discernible light-toned depiction. The visualization of this subunit was achieved through the utilization of the true color composite R4/G3/B2.

The terrace predominantly exhibits a green hue, attributed to the dense vegetation cover, with patches of brown where the soil is exposed. Whitish areas indicate a substrate with higher sand content, while blue hues depict drainage patterns, the adjacent sea, and enclosed water bodies (Figure 3). The DSM played a crucial role in defining the boundaries of this subunit, as the terrace's elevated position within the plain serves as a distinguishing factor, setting it apart from both the paleoestuarine zone and the external marine terrace (Figure 9).

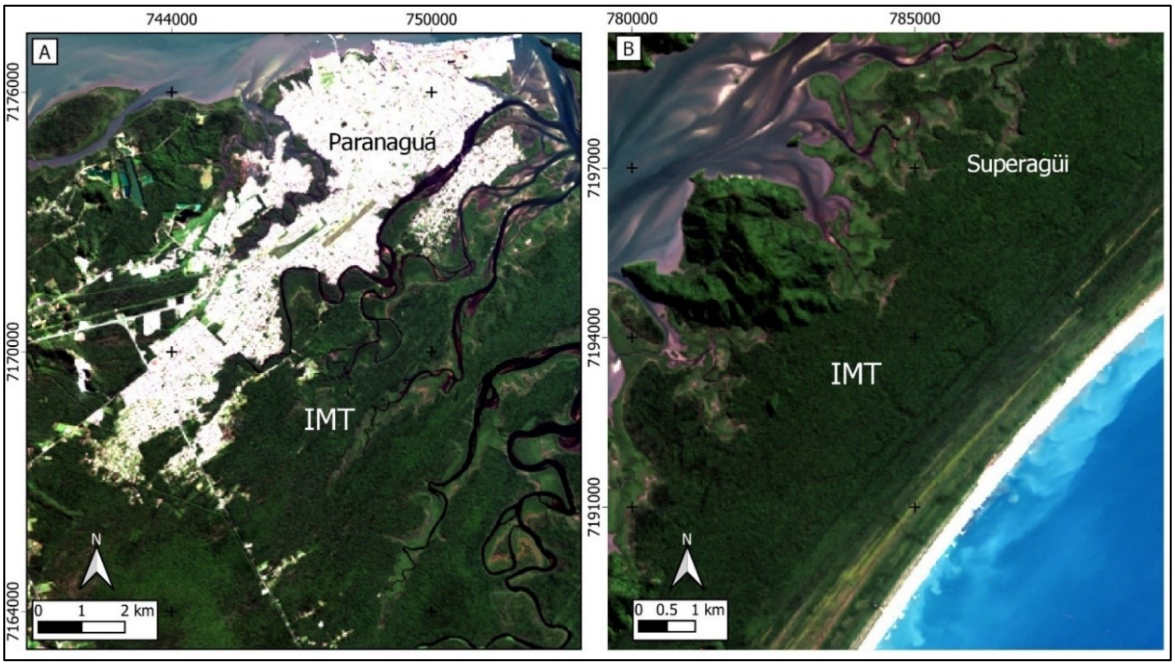

Figure 3. Internal marine terrace (IMT) showed by Landsat 8 true color composition R4/G3/B2 with linear contrast enhancement: A) Paranaguá strandplain and B) Superagüi strandplain.

External marine terrace (ETM)

Comprising Holocene sediments, the external marine terrace is notably discussed in papers by Angulo (1992), Souza et al. (2012), and Bogo et al. (2021). Its geographical presence is established at the periphery of the Paraná coastal plain (Figure 4). According to Martin et al., (1988) and Angulo and Lessa (1997) with the gradual sea level fall after the postglacial maximum, the terrace was formed 5000 years B.P. presenting altitudes between +2.5 m and +4 m, being topographically lower than the internal marine terraces. Bogo et al. (2023), illustrated very well these stages of Holocene barrier evolution correlating the dating and core descriptions. The beach ridges are present on this terrace, as well as adorning the internal marine terraces, however, unlike the old ridges, these are better delineated.

This subunit's visibility is manifest through multiple band compositions but presented here by the false color composition R6/G5/B2 (Figure 4). This composite displays a greenish tint where vegetation blankets the land (band 5 – near-infrared), contrasting with the rosy hue of exposed soil (band 6 – short wavelength infrared) while water bodies adopt a serene blue (band 2 – blue).

Beach ridges (BR)

The beach ridges on the external marine terrace exhibit notable clarity in their delineation, characterized by their linear, shore-parallel, and sub-parallel disposition (NE-SW orientation) shown in Figure 5. These ridges stand apart from one another by depressions made up of wetlands, swamps, and river courses (Angulo, 2004). These are indicators of the positions of ancient seashores, pointing to possible processes of relative sea level oscillations and coastline progradation (Otvos, 2000). In the Paranaguá strandplain, the ridges lineaments are more defined by the vegetation, and it is not possible to observe the land surface. In this region, it is possible to visualize the beach ridges through the radargram profile presented by Bogo et al. (2021).

Within the Superagüi strandplain, the lineaments have exposed soil and wetlands between the ridges. The visualization of the beach ridges was achieved through the use of the color composite R5/G4/B3 (Figure 5). In this composition, band 4 (red) effectively captures vegetation, appearing as a red hue, contrasting with the exposed soil portrayed in a cyan color through band 5 (near infrared). Band 3 (green) highlights wetlands, depicted in a green hue with relatively lower reflectance.

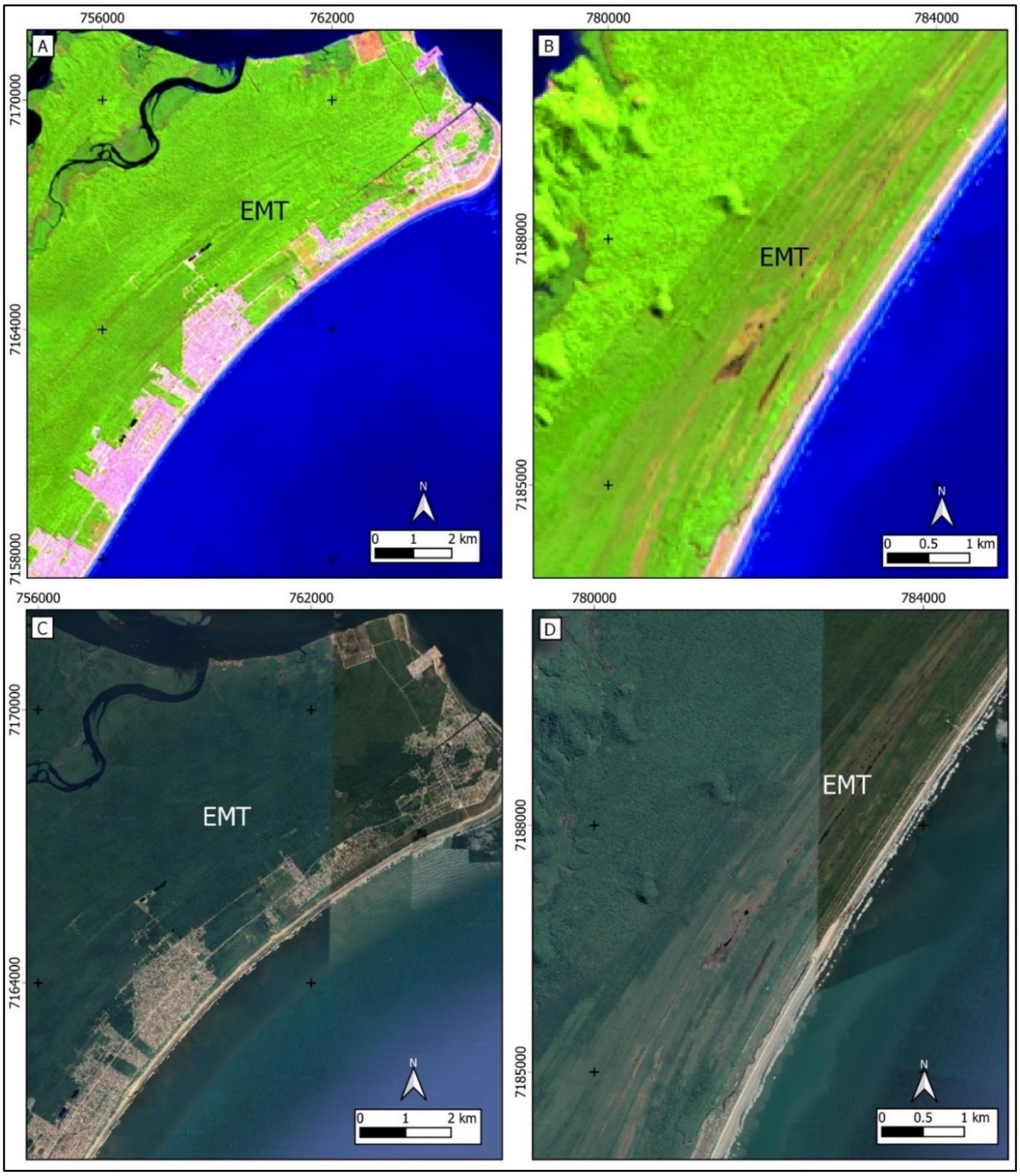

Figure 4. External marine terrace (EMT) showed by Landsat 8 color composite R6/G5/B2 with linear contrast enhancement: A) Paranaguá strandplain and B) Superagüi strandplain. Google earth image: C) Paranaguá strandplain and D) Superagüi strandplain.

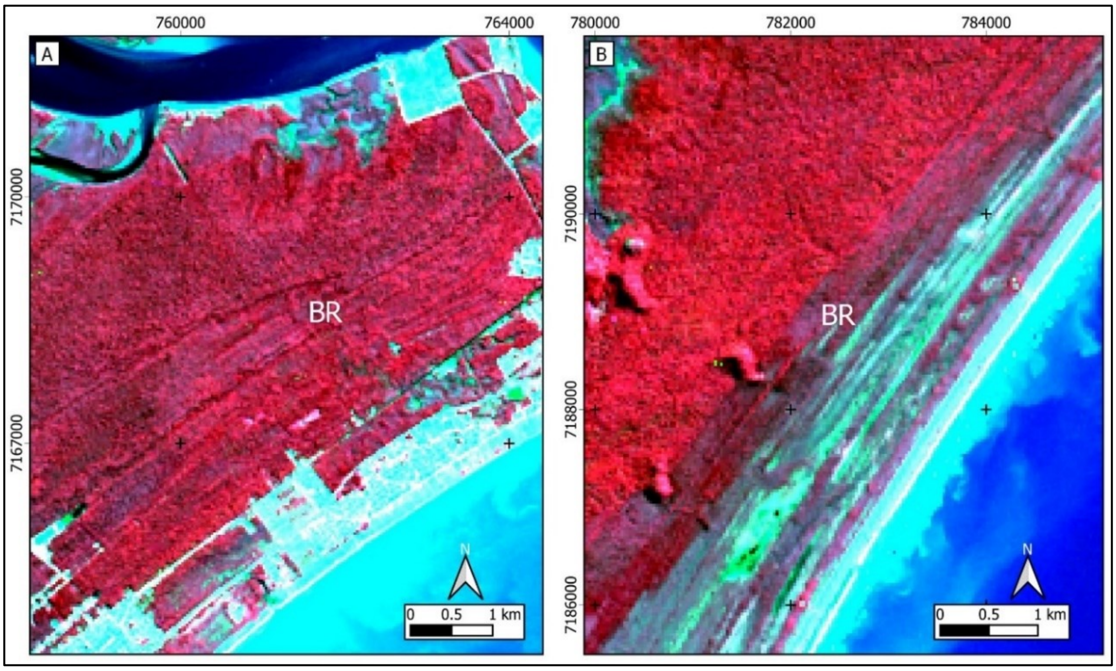

Figure 5. Beach ridges (BR) showed by Landsat 8 color composite R5/G4/B3 with linear contrast enhancement: A) Paranaguá strandplain and B) Superagüi strandplain.

Beach (BE)

The current beach manifests as a linear expanse along the coastline, characterized by devoid of vegetation, light-toned appearance, and notable reflectivity, primarily attributed to the prevalence of quartz sand (Figure 6). The beaches within the Paraná region are made up of fine to medium sand, well sorted, consisting mainly of quartz and variable levels of biodetrital carbonate fragments and heavy minerals (Bigarella et al., 1966, 1969a, 1970/71; Angulo et al., 1996). The beaches are wave-dominated along the open coast and tidally modified inside the estuaries (Angulo et al., 2016).

Although discernible in numerous color compositions, this particular class exhibited enhanced visibility through the application of the false color composite R7/G6/B5, as showcased in Figure 6. In this composite, areas with vegetation coverage adopt a bluish hue (band 7 - short wavelength infrared), exposed soil takes on a yellow tint, and zones abundant in quartz sand are depicted in white. Additionally, wetlands and water bodies are characterized by a deep blue tone.

Paleoestuarine plain (PP)

Predominantly situated within the topographic depression that spans between the internal and external terraces of the Paranaguá strandplain, this class also finds its presence in the lowland regions within the inner expanse of the Superagüi strandplain (Figures 9 and 10). According to Angulo et al., (2002), the dating of a trunk fragment found in the area showed an age beyond the reach of the 14C method (> 40000 years B.P., CENA-121), which allowed correlating the deposits to the transgressive-regressive cycle of the last interglacial in the Pleistocene. In Superagüi, the head of several paleo-streams incised in the Pleistocene plain are cut off, suggesting that the Holocene plain overstepped the Pleistocene one during the final phases of the post-glacial marine transgression (Lessa et al., 2000).

Sands stand as the dominant sediment constituents, accompanied by subsidiary occurrences of clayey sands, silty sands, and clayey-sandy silt. The sorting characteristics range from very well to very poorly sorted, as elucidated by Angulo (1992) and Angulo and Absher (1992). Across the paleoestuarine plain, pockets of floodplain terrain are interspersed around the meandering river channels. Nonetheless, discerning a distinct boundary between these two subunits was not clear in the satellite imagery. To enhance the visual representation of this class, a Google Earth image was also incorporated as illustrated in Figure 7. The color composite chosen to showcase the paleoestuarine plain comprised R5/G4/B3, wherein band 5 represented near-infrared, band 4 denoted red, and band 3 indicated green (Figure 7). This RGB composite yielded an image of the plain characterized by reduced reflectance and a darker hue due to its sedimentary composition.

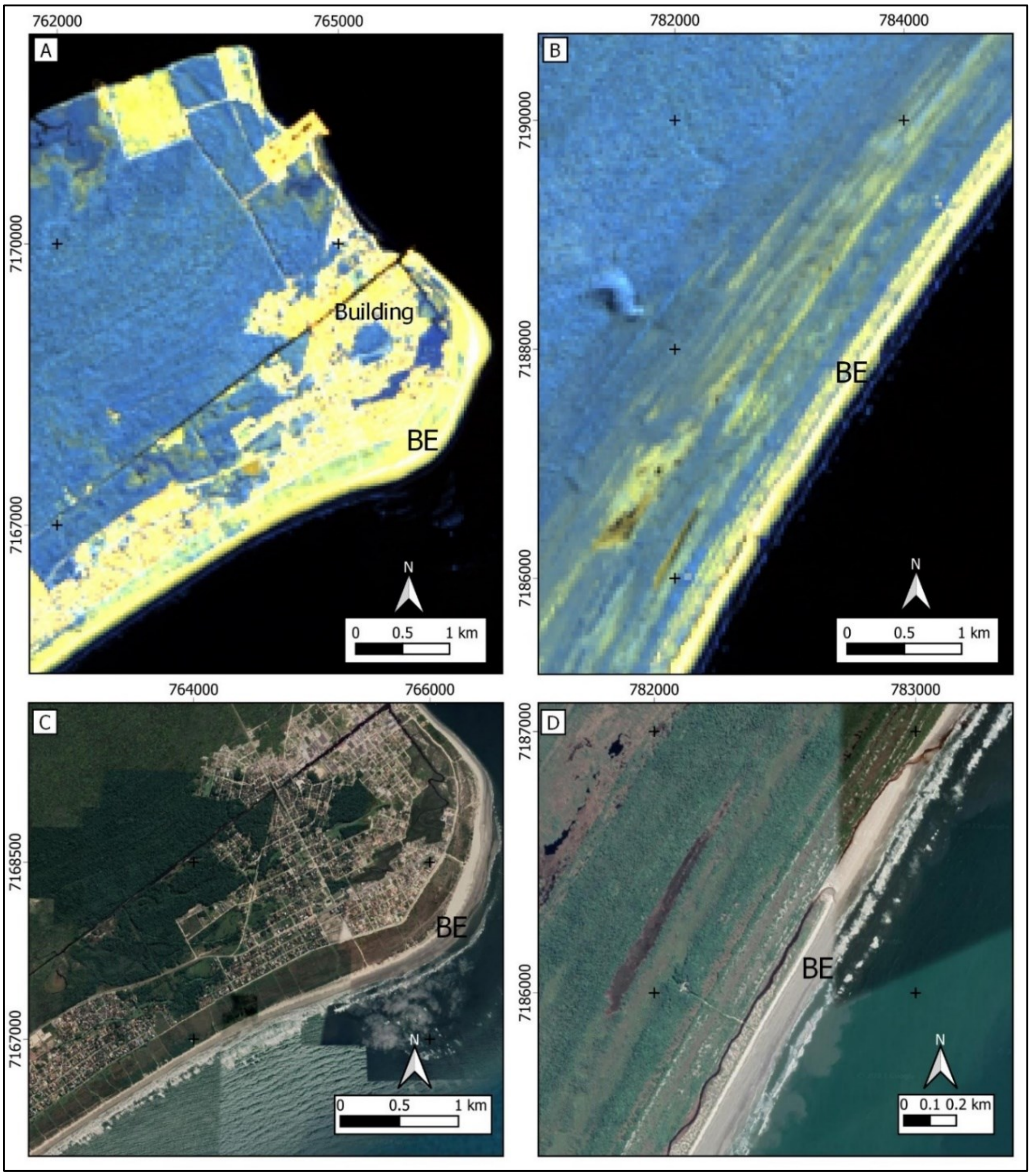

Figure 6. Beach (BE) showed by Landsat 8 color composite R7/G6/B5 with linear contrast enhancement: A) Paranaguá strandplain and B) Superagüi strandplain. Google earth image: C) Paranaguá strandplain and D) Superagüi strandplain.

Tidal flat/mangrove (MA)

This subunit takes form on terrain characterized by its flat and low-slope topography (Figures 9 and 10), shielded from the impact of vigorous wave action, and influenced by tidal forces. As several ecosystems occur in these areas, Angulo (1990) suggested the use of the name tidal flat and not just mangrove, since other five units occur together: marshes and non-vegetated banks, mangrove with *Acrostichum* and *Hibiscus*, *Cladium* zone, tidal marsh and tidal marsh. The sediments range from sands to sandy clays, are generally rich in organic matter, and may contain granules and pebbles (Bigarella, 1946; Martin et al., 1988; Angulo, 1992b). This subunit, tidal flat/mangrove, was also the subject of research by Comerlato et al. (2023), aiming at a separation with a morphometric signature. Therefore, the authors defined it as an estuarine plain and estuarine terrace through object-oriented supervised classification on RapidEye satellite image.

This class was identified in all remote sensing products analyzed, however according to Kuenzer et al. (2011), the spectral behavior of mangrove vegetation has low reflectance in the visible and a peak in the near-infrared. The best presentation in this subunit was the color composite R5/G6/B2 (Figure 8), due to a greater contrast of the plains with the vegetation and water with its surroundings. A distinct reddish and brown coloration of low reflectance is discernible (band 5 – near-infrared), which starkly contrasts with the orange-toned vegetation (band 6 – short wavelength infrared) and takes on a greenish hue at feature intersections. Additionally, bodies of water are characterized by shades of blue and black (band 2 – blue).

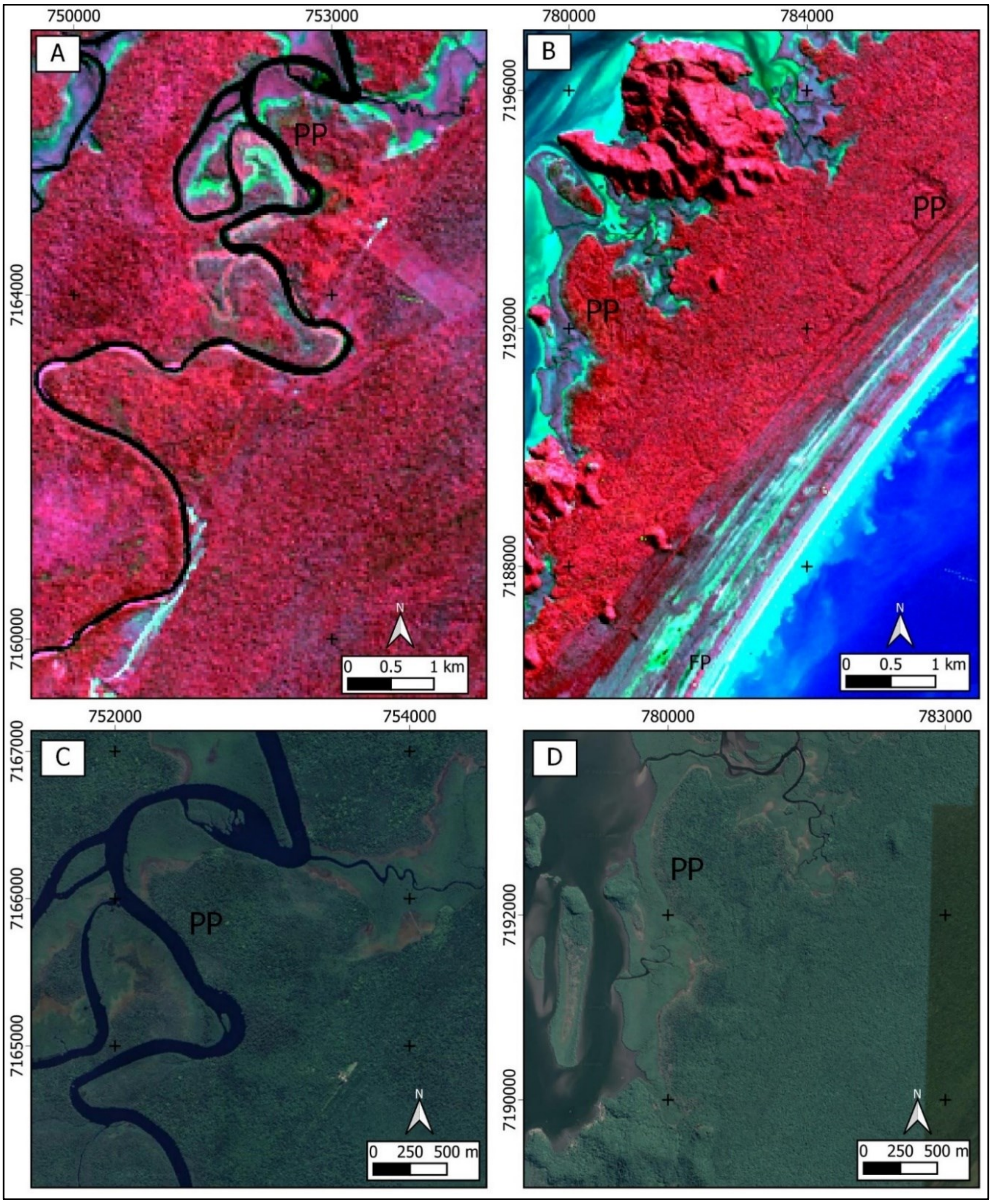

Figure 7. Paleoestuarine plain (PP) showed by Landsat 8 color composite R5/G4/B3 with linear contrast enhancement: A) Paranaguá strandplain and B) Superagüi strandplain. Google earth image: C) Paranaguá strandplain and D) Superagüi strandplain.

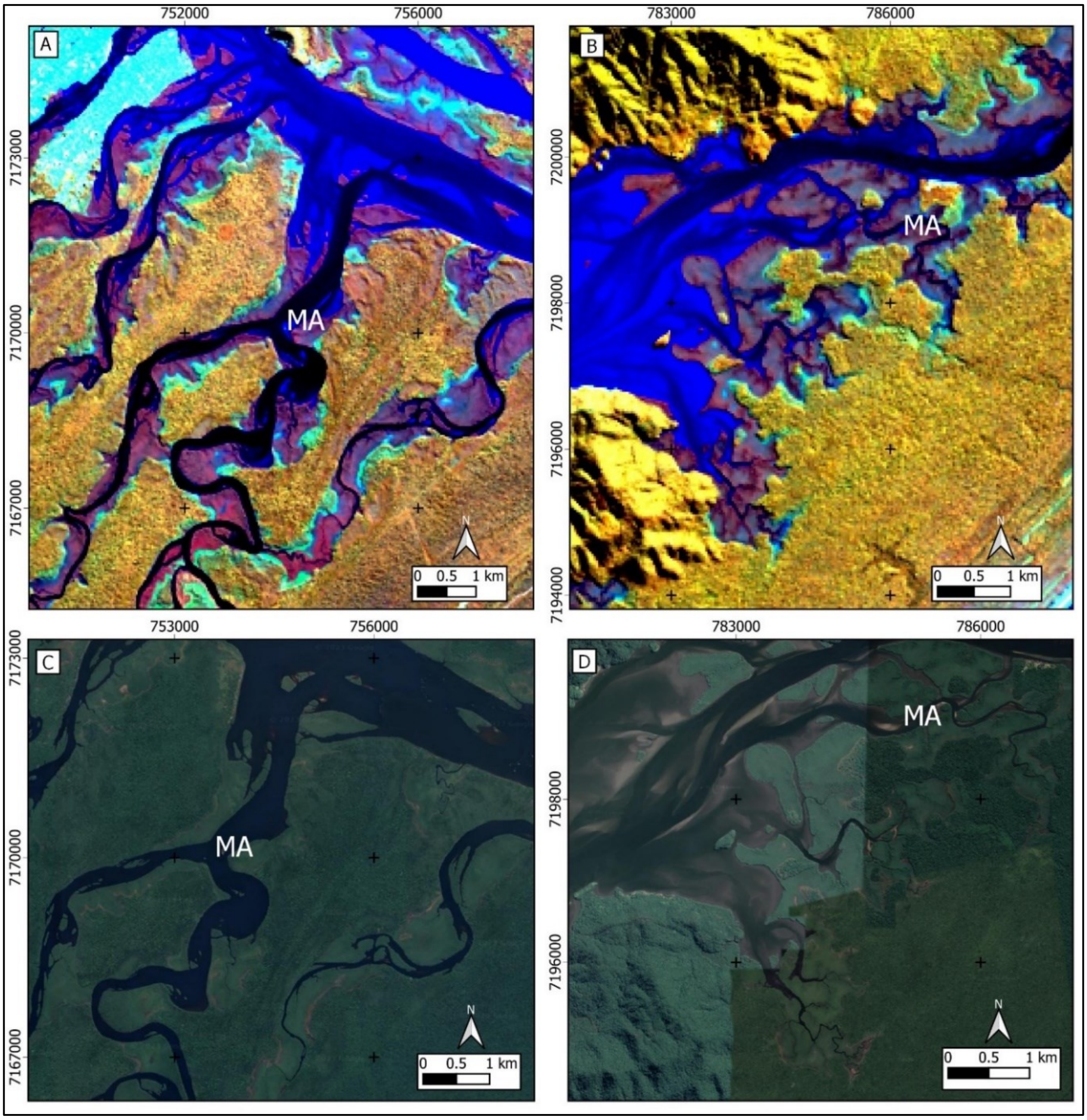

Figure 8. Tidal flat/mangrove (MA) showed by Landsat 8 color composite R5/G6/B2 with linear contrast enhancement: A) Paranaguá strandplain and B) Superagüi strandplain. Google earth image: C) Paranaguá strandplain and D) Superagüi strandplain.

Relief analysis

The region's morphology displays heterogeneity, with notable topographical variations between the examined units and subunits (as Figures 9 and 10). Altitude and slope maps unveiled a relief marked by low elevations and a distribution of slopes ranging from 0° to 5°, except for the crystalline basement locations, where the highest altitudes and steeper slopes exceeding 10° were observed (Figures 9a, 9b and 10a, 10b). From the intersection of RGB attributes, areas with higher altitudes and slopes are represented by the yellow color, as it was possible to observe the crystalline basement presence in both strandplains, presenting a steeper morphology (Figures 9d and 10d).

Overall, the strandplains exhibit a topography ranging from flat to gently undulating, with the most pronounced topographical variations evident between the beach ridges and at the boundaries of the barriers. These barriers are distinctly demarcated between the internal and external marine terraces, as evidenced in the optical images. However, upon analyzing the RGB composite, regions characterized by medium to high altitudes and specific azimuth orientations tend to be predominantly represented by a dominant pink color (Figures 9d and 10d). Thus, the internal marine terrace (Pleistocene ages – barriers II and III) showed a greater elevation compared to external marine terrace (Holocene age - barrier IV), also corroborating with the altitude map and topographic profile (Figures 9a, 9e and 10a, 10e) that show a progressive decline of the topography towards the coastline (Angulo et al., 2004; Guedes et al., 2020; Comerlato et al., 2023). In both the altitude and RGB composite representations, the topographic depression, corresponding to the paleoestuarine plain in the optical images, becomes discernible. Areas with lower altitudes, gentle slopes, and orientations towards higher azimuths tend to manifest as shades of cyan color as shown in Figures 9 and 10. This observed trend was particularly pronounced at the boundary between the two terraces and the adjacent paleoestuarine and mangrove regions. The greenish tone shows the contrast between the terraces and tidal flat/mangrove, accentuating the existing slope in the area and corroborating with the slope map that shows this border represented by the red color.

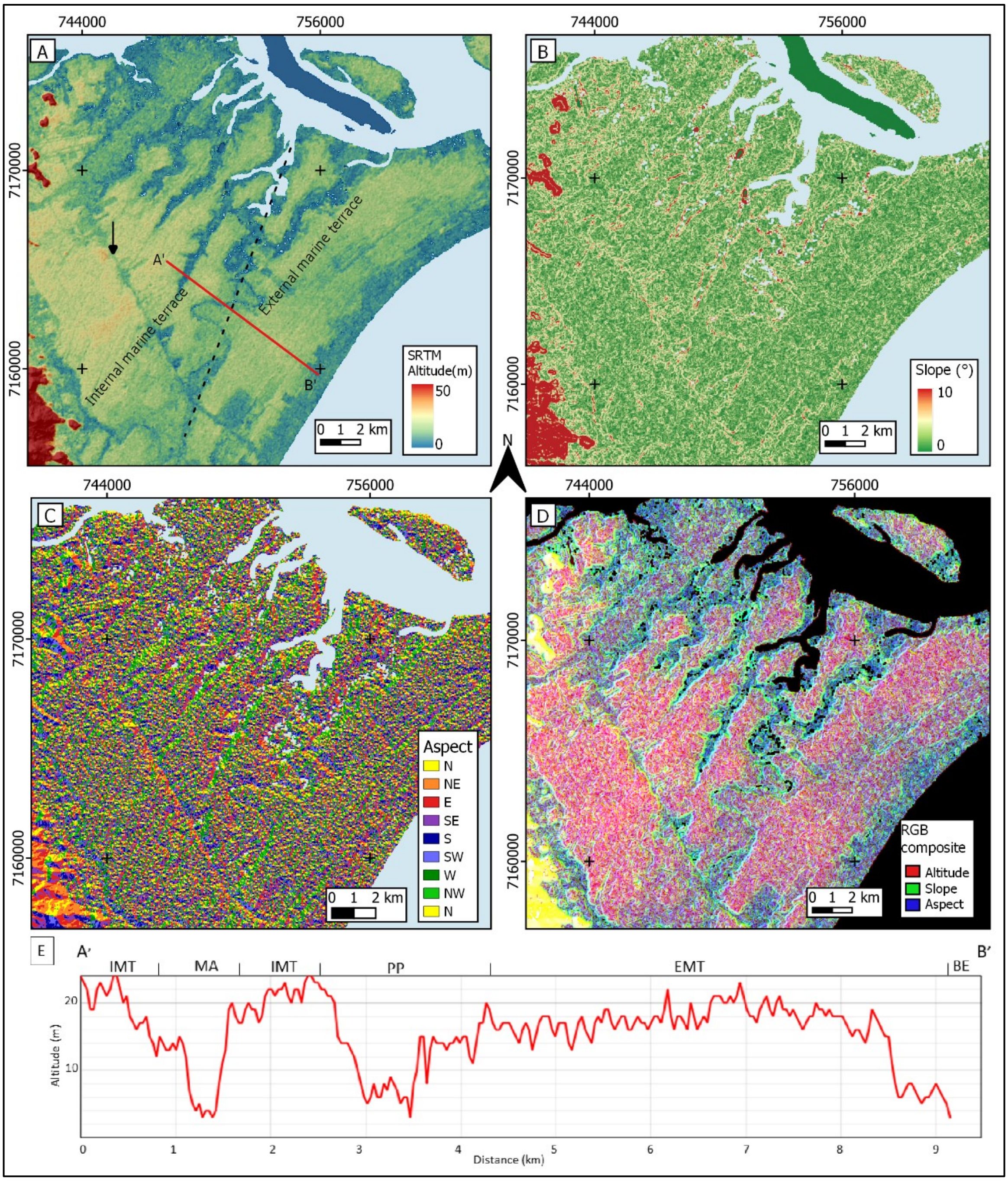

Figure 9. Paranaguá Digital Surface Model and derived products: A) altitude, B) slope, C) aspect, and D) RGB composite; E) topographic profile (A'- B') obtained from the MDS-SRTM data with indication of the position of each subunit. Observation: the black arrow indicates an urban road.

The aspect map revealed a landscape characterized by elongated features, with the steepest slopes oriented towards the southeast (Figures 9c and 10c). The alignment of these features, accentuated by the ridges, manifests a prevailing pattern of orientation from NE-SW. This distinctive pattern is prominently displayed across all the products. This map also corroborates the features analyzed in the optical image that allowed the defining of the beach ridges subunit. Within the Superagüi strandplain, a distinct linear feature becomes apparent in the central expanse of the internal marine terrace (Pleistocene age - barrier III), denoting a sharp change in the maximum NW ward slope. Correspondingly, the altitude map corroborates this observation by manifesting a noticeable topographic elevation. Given the dense vegetation that shrouds the barrier, visual identification of this feature poses a challenge, making subsurface field studies recommended for further investigation.

The topographic profiles reveal a gradual decline in altitude from the inner portion of the terrace towards the coast (Figures 9e and 10e).

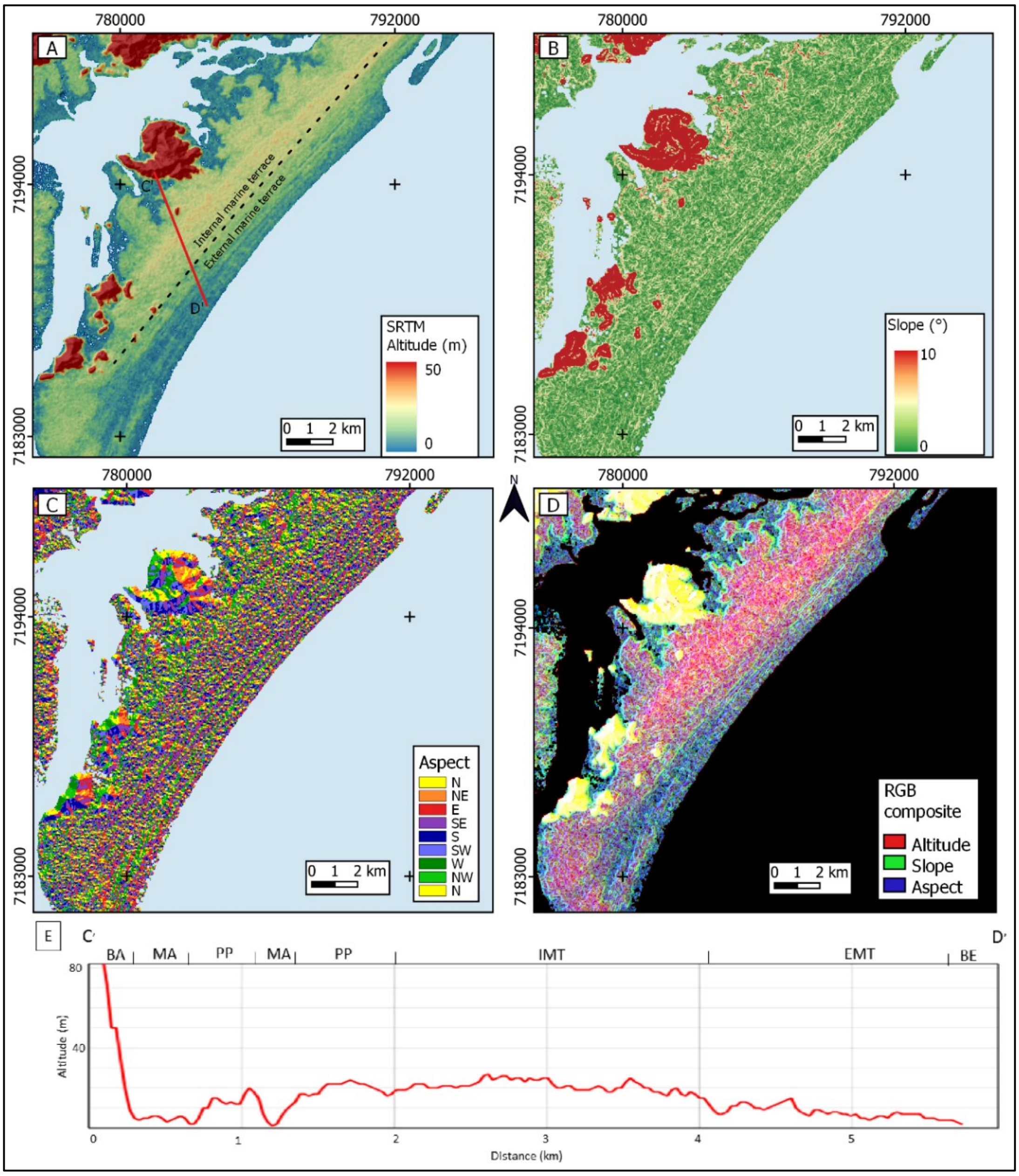

Figure 10. Superagüi Digital Surface Model and derived products: A) altitude, B) slope, C) aspect, and D) RGB composite; E) topographic profile (C'- D') obtained from the MDS-SRTM data with indication of the position of each subunit.

This descent becomes even more apparent through the presence of a distinct bluish hue in the RGB composite map, serving as an indicator of lower elevation levels (Figures 9d and 10d). It is important to note that the topographical values are higher than what is presented in the literature (Lessa et al., 2000; Angulo et al., 2006a; Angulo et al., 2009). The discrepancy in numbers occurs due to vegetation, which changes the position of maximum elevations in the SRTM data, corroborating Angulo (1992). The author highlights an interesting observation regarding the vegetation's altitude surpassing that of the terrain's slope, with an inversion of numbers and adding high stretches where the terrain would be lower.

A remarkably distinct geomorphic attribute, situated at a lower elevation, is easily discernible as it traverses across the entirety of the Paranaguá strandplain. This is indicated by a prominent black arrow as illustrated in Figure 9a. This distinctive feature corresponds to a thoroughfare constructed within the locale, drawing distinct attention to cartographic representations due to the absence of vegetative cover in the immediate vicinity. This absence is an outcome of the Digital Surface Model (DSM) methodology, which includes the uppermost portions of tree canopies in its representation of the topography.

Consequently, it became evident that the derived outputs from SRTM data (Figures 9 and 10) significantly enhanced the differentiation of the various geomorphological units that constitute the coastal region. This, in turn, greatly facilitated the morphological distinction of each subunit as visualized in the optical images (e.g., Nelson et al., 2009; Ghoneim et al., 2012; Zhang et al., 2020). Rosa et al. (2017) characterized the Lagoon-Barrier Systems II, III, and IV in the Rio Grande do Sul plain through elevation steps using the RGB composite map, revealing distinct altitudes among the barriers and lagoons present. In this study, a notable distinction was achieved between the older terrace of the Pleistocene age, characterized by elevated altitudes and steeper slopes, and the younger terrace of the Holocene age, encompassing lower elevation regions and marked by a prominent occurrence of beach ridges. This finding further supports the similarity of deposits in other plains formed during sea level rise events (e.g., Suguio et al., 1985; Angulo and Lessa, 1997; Dillenburg and Hesp, 2009; Angulo et al., 2009; Ramos et al., 2021).

Bogo et al. (2023), also processed an altitude map of the Paranaguá strandplain, however, using the Alos Palsar Digital Elevation Model data. The map corroborates what was done in this research, where it shows the differentiation between the terraces, with higher elevations, and the tidal flat and beach environments, with lower elevations, also supporting what was reported by Rosa et al. (2017).

Geomorphological mapping

The integration of visual interpretation involving Landsat 8 optical images, SRTM data products, Google Earth imagery, and geological maps facilitated the distinct identification and cartographic representation of the geomorphological subunits within the Paranaguá and Superagüi strandplains at a scale of 1:100,000. This was achieved using QGIS® 3.16 software represented in the following Figures 11 and 12.

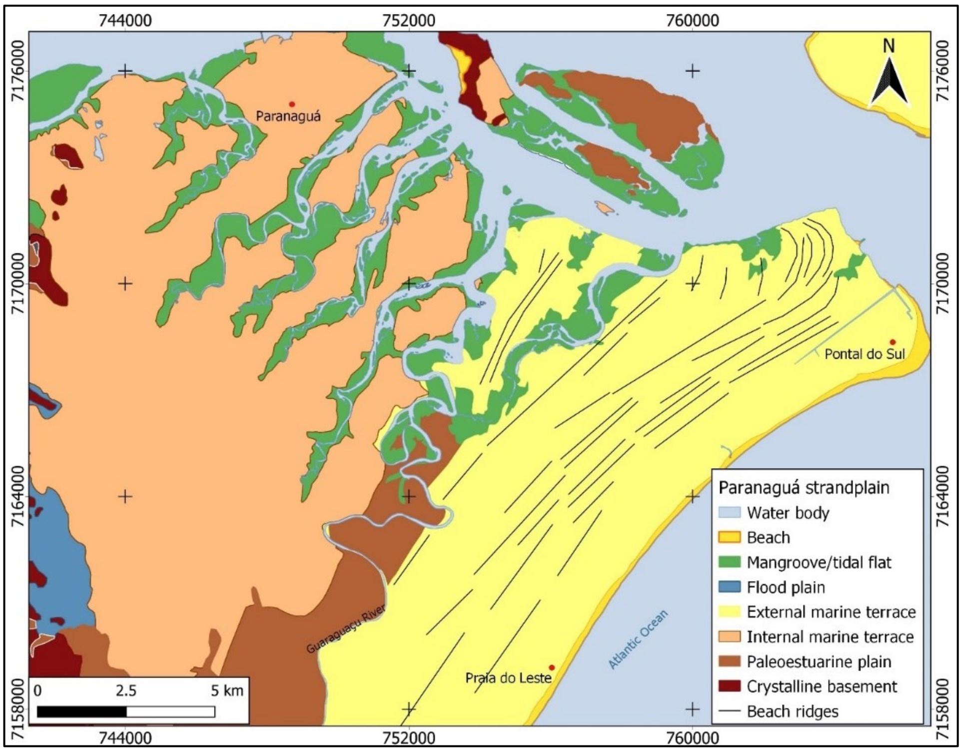

Figure 11. Geomorphology map of the Paranaguá strandplain.

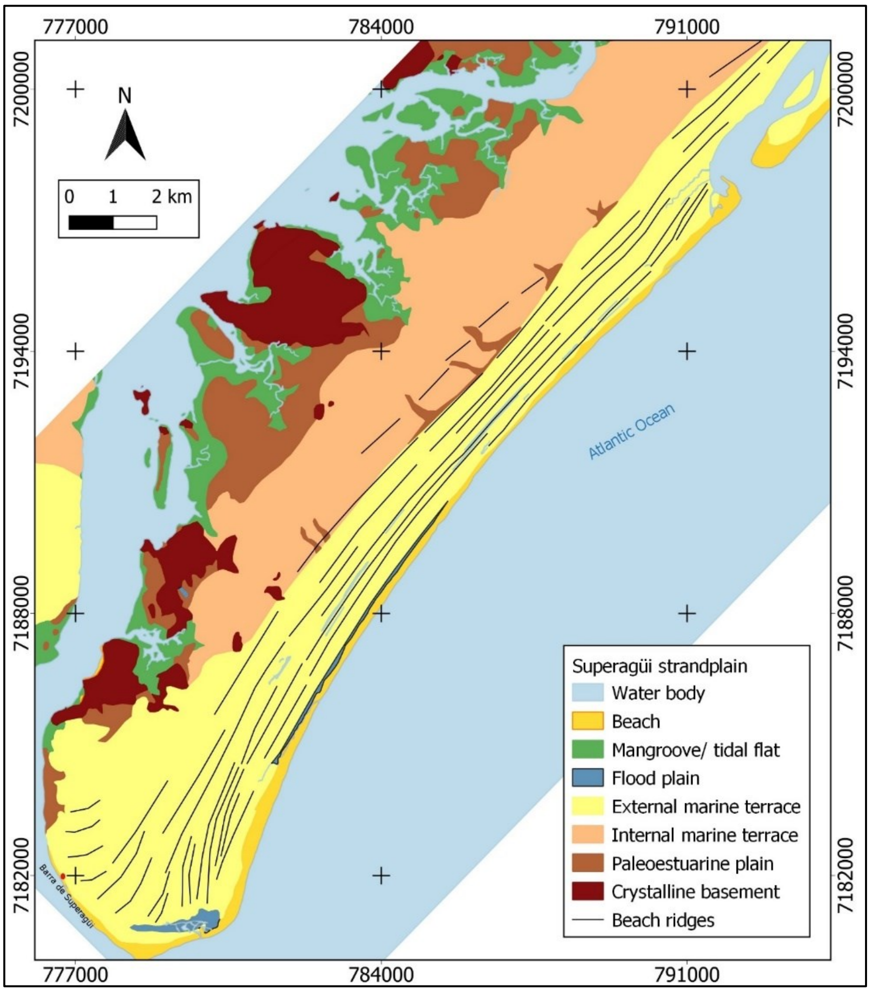

Figure 12. Geomorphological map of the Superagüi strandplain.

Conclusions

The combined use of remote sensing and GIS analysis techniques proved efficient in interpreting coastal landscape features and depositional environments, resulting in the successful production of geomorphological maps.

The analysis revealed that the diversity of morphological and sedimentological characteristics in coastal deposits exhibited unique reactions for each observed subunit, which were expressed through variations in color, texture, and relief. This phenomenon was particularly evident within the context of image digital processing and digital surface model analysis.

By applying digital processing and analysis to optical images, using color composites such as R4/G3/B2, R6/G5/B2, R5/G4/B3, R7/G6/B5, and R5/G6/B2, the study effectively delineated the primary geomorphological units and subunits present in Landsat 8 OLI images. It is important to note that alternative combinations of spectral bands can also be utilized for analysis, mapping, and the demarcation of coastal features. Additionally, the data provided by SRTM, MDS, and related products, facilitated the exploration of topographical variations within the strandplains, particularly in regions like the paleoestuarine plain and marine terraces.

The integration of remote sensing techniques with other methodologies proved to be an indispensable asset in coastal evolution research, especially for identifying and demarcating features linked to coastal barriers and their adjacent deposits. The generated maps hold significant value in streamlining research efforts, effectively optimizing study time by aiding in the delineation of research areas and providing clearer, more precise targets for investigation.

Despite the spatial distribution and morphological characteristics of the plains presented, it is suggested future research involving subsurface data acquisition in the region, mainly in the inner portion, is carried out. This approach would enable visualization of the substrate and provide a comprehensive understanding of the formation and evolution of the existing Pleistocene and Holocene terraces.

Acknowledgment

The authors wish to thank the Coordination for the Improvement of Higher Education Personnel (CAPES) for granting the scholarship, the National Council for Scientific and Technological Development (CNPq) for financial support, the post-graduate research program and Laboratory of Coastal Studies (LECOST) of Federal University of Paraná for assistance, knowledge and equipment used in the field.

References

Angulo, R.J., 1990. O manguezal como unidade dos mapas geológicos. In: Simp. Ecoss. Costa Sul Sudeste Bras., 2. Águas de Lindóia. São Paulo, ACIESP. 2, 54-62.

Angulo, R. J., 1992. Geologia da Planície Costeira do Estado do Paraná. Instituto de Geociências, Universidade de São Paulo, São Paulo, Tese de Doutoramento, 334 p. (Biblioteca do Centro Politécnico da UFPR).

Angulo, R.J., 1992b. Geologia da Planície Costeira do Estado do Paraná. Inst. de Geociências, Universidade de São Paulo, São Paulo, Tese de Doutorado. 334 p.

Angulo, R.J., Absher, T.M. 1992. Sedimentos paleoestuarinos da planície costeira do Estado do Paraná. Bol. Par. Geoc. Curitiba. 40, 115-135.

Angulo, R.J, 1993. Morfologia e gênese das dunas frontais do litoral do estado do Paraná. Revista Brasileira de Geociências. 23(1), 68-80.

Angulo, R.J., Suguio, K., 1995. Re-evaluation of the Holocene sea-level maxima for the State of Paraná, Brazil. Paleogeography, Palaeoclimatology, Palaeoecology. 113(2–4), 385–393. https://doi.org/10.1016/0031-0182(95)00055-Q.

Angulo R.J., Giannini, P.C.F., Kogut, J.S., Prazeres, F.H.J., Souza, M.C., 1996. Variação das características sedimentológicas através de uma sucessão de cordões litorâneos holocênicos na ilha do Mel, Estado do Paraná. Bol. Par. Geoc. Curitiba. 44, 77-86

Angulo, R.J., Lessa, G.C., 1997. The Brazilian Sea level curves: a critical review with emphasis on the curves from Paranaguá and Cananéia regions: Marine Geology. 140, 141–166. https://doi.org/10.1016/S0025-3227(97)00015-7

Angulo, R.J., Pessenda, L.C.R., Souza, M.C., 2002. O significado das datações ao 14C na reconstrução de paleoníveis marinhos e na evolução das barreiras quaternárias do litoral paranaense. Rev. Bras. Geociências. 32 (1), 95-106.

Angulo, R.J, 2004. Mapa do Cenozóico do litoral do Estado do Paraná. Boletim Paranaense de Geociências. 55 (1), 16-30.

Angulo, R.J., Lessa, G.C., Souza, M.C., 2006a. A critical review of mid-to late Holocene sea-level fluctuations on the eastern Brazilian coastline. Quat Sci Ver. 25, 486–506

Angulo, R.J., Souza, M.C., Assine, M.L., Pessenda, L.C.R., Disaró, S.T., 2008. Chronostratigraphy and radiocarbon age inversion in the Holocene regressive barrier of Paraná, southern Brazil. Marine Geology. 252 (3–4), 111–119. https://doi.org/10.1016/j.margeo.2008.03.006.

Angulo, R.J., Lessa, G.C., Souza, M.C., 2009. The Holocene Barrier Systems of Paranaguá and Northern Santa Catarina Coasts, Southern Brazil, in: Dillenburg, S.R., Hesp, P.A. (Eds.), Geology and Geomorphology of Holocene Coastal Barriers of Brazil.135–176.

Angulo, R.J., Souza, M.C., Noernberg, M.A., Borzone, C.A., Quadros, C.J.L., Rosa, L.C., 2016. The State of Parana beaches. In: Short, A.D., Klein, A.H.F. (Eds.), Brazilian Beach Systems. Springer, pp. 419–460.

Benavente, J., Ruiz de Alegrıa-Arzaburu, A., Plomaritis, T.A., Sedrati, M., Ariffin, E.H., 2023. Editorial: Coastal environment in a changing world. Front. Mar. Sci., v. 10, 1213689. doi: 10.3389/fmars.2023.1213689.

Bigarella, J.J., 1946. Contribuição ao estudo da planície litorânea do estado do Paraná. Arquivos de Biologia e Tecnologia. 1, 75–111.

Bigarella, J.J., Freire, S.S., Salamuni, R., Viana, R., 1966. Contribuição ao estudo dos sedimentos praiais recentes, II Praias de Matinhos e Caiobá. Bol. Univ. Fed. Par. Geog.Fís., Curitiba. 6, 109.

Bigarella, J.J., Alessi, A.H., Becker, R.D., Duarte, G.K., 1969a. Textural characteristics of the coastal dune, sand ridge, and beach sediments. Bol. Par. Geoc., Curitiba. 27, 15-80.

Bigarella, J.J., Duarte, M.G., Becker, R.D., 1970/71. Structural characteristics of the dune, foredune, interdune, beach, beach-dune ridge and sand ridge deposits. Bol. Par. Geoc., Curitiba. 28-29,9-72.

Bigarella, J.J., 1971. Variações climáticas no Quaternário Superior do Brasil e sua datação radiométrica pelo método do Carbono 14. Paleoclimas Inst. Geogr. USP. 1, 1-22.

Bishop-Taylor, R., Nanson, R., Sagar, S., Lumburner, L., 2021. Mapping Australia's dynamic coastline at mean sea level using three decades of Landsat imagery. Remote Sensing of Environment. 262 (1): 112734. doi:10.1016/j.rse.2021.112734

Biswas, R. N., Rashid, K. J., Jahan, Md. N., Chowdhury, Md. N. A., 2024. Geomorphological changes and landscape ecosystem services dynamics of the Bhasan Char Island in the Northern Bay of Bengal, Bangladesh. Ocean & Coastal Management, v. 252, 1,107096. https://doi.org/10.1016/j.ocecoaman.2024.107096.

Bogo, M., Nascimento, M.G., Souza, M.C, Angulo, R. J., Guedes, C.C.F., Rosa, M.L. C.C., Barboza, E.G., 2021. Spit-Inlet migration and storm-driven stacking at Praia de Leste Holocene barrier, southern Brazil. Marine Geology. 422, 106637. https://doi.org/ 10.1016/j.margeo.2021.106637.

Bogo, M., Souza, M.C., Angulo, R.J., Barboza, E.G., Rosa, M.L.C.C., Caron, F., Junior, A.L.F., Santos, S.F., 2023. Inlet migration during the turning point between transgressive and regressive stages at the Guaratuba Holocene barrier, Paraná - Southern Brazil. Marine Geology. 459, 107048. https://doi.org/10.1016/j.margeo.2023.107048.

Butler, D. R., Walsh, S. J., 1998. The application of remote sensing and geographic information systems in the study of geomorphology: An introduction. Geomorphology. 21(3), 179-181. https://doi.org/10.1016/S0169-555X(97)00056-1.

Chen, J., Wang, Y., Wang, J., Zhang, Y., Xu, Y., Yang, O., Zhang, R., Wang, J., Wang, Z., Lu, F., Lu, Z., 2024. The Performance of Landsat-8 and Landsat-9 Data for Water Body Extraction Based on Various Water Indices: A Comparative Analysis. Remote Sens. 16 (11), 1984. https://doi.org/10.3390/rs16111984.

Comerlato, T., Lamour, M.R., Silveira, C.T., 2023. Proposta metodológica para a classificação de unidades de relevo na porção central da planície costeira do Paraná -Brasil. Revista Brasileira de Geomorfologia, v.24 n.4; DOI: http://dx.doi.org/10.20502/rbg.v24i4.2395

Cowell, P.J., Thorn, E. G., 1994. Morphodynamics of coastal evolution. In: Carter, R.W.G., Woodroffe, C.D., (Ed). Coastal evolution: Late Quaternary shoreline morphodynamics. 511p.

Davis, Jr. R., FitzGerald, D., 2004. Beaches and Coasts. Blackwell Science Ltd, UK.

Dillenburg, S. R., Hesp, P. A., 2009. Coastal Barriers – An Introduction. Geology and Geomorphology of Holocene Coastal Barriers of Brazil. Lecture Notes in Earth Sciences. Springer. Berlin. 107.

Florenzano, T. G., 2007. Iniciação em sensoriamento remoto – 2ed, Oficina de textos.

Ghoneim, E., Benedetti, M., El-Baz, F., 2012. An integrated remote sensing and GIS analysis of the Kufrah Paleoriver, Eastern Sahara. Geomorphology. 139-140, 242-257. https://doi.org/10.1016/j.geomorph.2011.10.025.

Giaccone, E., Oriani, F., Tonini, M., Lambiel, C., Mariéthoz, G., 2022. Using data-driven algorithms for semi-automated geomorphological mapping. Stoch Environ Res Risk Assess 36, 2115–2131. https://doi.org/10.1007/s00477-021-02062-5.

Griffiths, J. S.; Abraham, J. K., 2008. Factors affecting the use of applied geomorphology maps to communicate with different end-user. Journal of maps, p. 201-210. doi:10.4113/jom.2008.89

Guedes, C.C.F., Nascimento, M.G., Angulo, R.J., Souza, M.C., 2020. Geological evidences as a guide to OSL dating interpretation and northern occurrence of MIS 7e barrier at Southern Brazil. Journal of South American Earth Sciences. 98,102478. https://doi.org/10.1016/j.jsames.2019.102478.

Hansen, M.A.F., Lima, J.P.R., Weschenfelder, J., Gruber, N.L.S., Moreira, C.A., 2021. Remote sensing and geology in the Bojuru region, middle portion of the Coastal Plain of Rio Grande do Sul State, Brazil: Boundaries of the Pleistocene and Holocene barriers and the forms of land use. Quaternary and Environmental Geosciences. 12(2), 55-64. http://doi.org/10.5380/abequa.v12i2.73379.

IBGE - Instituto Brasileiro de Geografia e Estatística, 2009. Manual técnico de geomorfologia. 2ed. Rio de Janeiro.

IPARDES – Instituto paranaense de desenvolvimento econômico e social, 1990. Macrozoneamento da APA de Guaraqueçaba. Curitiba, 2, 257.

Jensen, J. R., 2009. Sensoriamento Remoto do Ambiente: uma perspectiva em Recursos Terrestres. Tradução de J. C. N. Epiphanio. São José dos Campos, SP. (Prentice Hall Series in Geographic Information Science. Tradution of: Remote Sensing of the environment: an Earth resource perspective.

Kawakubo, F.S., Morato, R.G., Nader, R.S., Luchiari, A., 2011. Mapping changes in coastline geomorphic features using Landsat TM and ETM+ imagery: examples in southeastern Brazil. International Journal of Remote Sensing. 32(9), 2547-2562. https://doi.org/10.1080/01431161003698419.

Kuenzer, C., Bluemel, A., Gebhardt, S., Vo Quoc, T., Dech, S., 2011. Remote Sensing of Mangrove Ecosystems: A Review. Remote Sensing. doi:10.3390/rs3050878.

Leal, R.A., Barboza, E.G., 2016. Caracterização geológica, geomorfológica e evolutiva holocênica do litoral sul de Jaguaruna, SC, Brasil. Pesquisas em Geociências. 43 (1), 417-430. https://doi.org/10.22456/1807-9806.83265.

Lessa, G.C., Angulo, R.J., Giannini, P.C.F., Araújo, A.D., 2000. Stratigraphy and Holocene evolution of a regressive barrier in south Brazil. Marine Geology. 165(1-4), 87-108. https://doi.org/10.1016/s0025-3227(99)00130-9.

Liang, S., 2001. Atmospheric Correction of Landsat ETM+ Land Surface Imagery—Part I: Methods. IEEE Transactions on geoscience and remote sensing. 39, 11. https://doi.org/10.1109/36.964986.

LIMA, S. de A.; VIEIRA, V. de C. B., 2024. Space-time analysis of land use and cover in the expansion of sugarcane agriculture in the municipality of Aldeias Altas, Maranhão, Brazil. Research, Society and Development. v. 13, n. 1. DOI: 10.33448/rsd-v13i1.44805.

Lopes, R.P., Kunoshita, A., Baffa, O., Figueiredo, A. M. G., Dillenburg, S. R., Schultz, C. L., Pereira, J.C., 2014. ESR dating of Pleistocene mammals and marine shells from the coastal plain of Rio Grande do Sul state, southern Brazil. Quaternary International. 352(C), 124-134.

Lu, L., Qureshi, S., Li, Q., Chen, F., Shu., L., 2022. Monitoring and projecting sustainable transitions in urban land use using remote sensing and scenario-based modelling in a coastal megacity. Ocean & Coastal Management, v. 224, 1, 106201. https://doi.org/10.1016/j.ocecoaman.2022.106201.

Machado, G., Pinto, M.L.C., 2017. Morfologia e processos de sedimentação: contribuições ao planejamento do uso da terra no litoral paranaense. Terra Plural. 11 (2), 254-270.

Mao, Y., Harris, D.L., Xie, Z., Phinn, S., 2022. Global coastal geomorphology – integrating earth observation and geospatial data. Remote Sensing of Environment. 278, 113082. https://doi.org/10.1016/j.rse.2022.113082.

Meneses, P. R., Almeida, T., 2012. Introdução ao processamento de imagens de sensoriamento remoto. Brasília, UnB. p.266.

Munasinghe, T. N., Warnasuriya, T. W. S., 2023. Spatiotemporal behaviour of shorelines due to natural and anthropogenic influences on the Dehiwala-Mt. Lavinia Beach, Sri Lanka: Insights towards effective application of satellite-derived data and geospatial techniques. Ocean & Coastal Management, v. 242, 106734. https://doi.org/10.1016/j.ocecoaman.2023.106734.

Nelson, A., Reuter, H.I., Gessler, P., 2009. Chapter 3 DEM production methods and sources. T. Hengl, H.I. Reuter (Eds.), Developments in Soil Science, Elsevier. 33, 65-85. https://doi.org/10.1016/S0166-2481(08)00003-2.

Otvos, E.G., 2012. Coastal barriers - Nomenclature, processes, and classification issues. Geomorphology. 139-140, 39–52. https://doi.org/10.1016/j.geomorph.2011.10.037.

Otvos, E.G., 2020. Coastal barriers - fresh look at origins, nomenclature and classification issues. Geomorphology. 355,107000. https://doi.org/10.1016/j.geomorph.2019.107000.

Peter, J, 2015. https://www.nv5geospatialsoftware.com/Learn/Blogs/Blog-Details/ArtMID/10198/ArticleID/15691/The-Many-Band-Combinations-of-Landsat-8 (accessed 12 August 2023).

Polizel, S. P., Rosseti, D. F., 2014. Caracterização morfológica do delta do Rio Doce (ES) com base em análise multissensor. Revista Brasileira de Geomorfologia. 15(2), 311-326. https://doi.org/10.20502/rbg.v15i2.530.

Quesada-Román, A.; Peralta-Reyes, M., 2023. Geomorphological Mapping Global Trends and Applications. Geographies, 3, 610–621. https://doi.org/10.3390/geographies3030032.

Radaideh, O.M.A., Grasemann, B., Melichar, R., Mosar, J., 2016. Detection and analysis of morphotectonic features utilizing satellite remote sensing and GIS: An example in SW Jordan. Geomorphology. 275, 58-79. http://dx.doi.org/10.1016/j.geomorph.2016.09.033

Ramos, L.P., Andrade, A.C.S., Nascimento, P.S.R., Santos, J.P.S., 2021. Mapeamento geomorfológico da zona costeira sul de Sergipe, nordeste do Brasil. Pesquisas em Geociências. 48(3), 107654.

Rodrigues, S. C., Augustin, C. H. R. R., & Nazar, T. I. S. M., 2023. Mapeamento Geomorfológico do Estado de Minas Gerais: uma proposta com base na morfologia. Revista Brasileira de Geomorfologia, 24(1). https://doi.org/10.20502/rbg.v24i1.2233

Rosa, M.L.C.C., Barboza, E.G., Tomazelli, L.J., Ayup-Zouain, R.N., Dillenburg S.R., 2007. Aplicação de Ferramentas de Visualização Tridimensional na Modelagem Geomorfológica da Região Sul da Província Costeira do Rio Grande do Sul. Gravel. 5, 1-10.

Rosa, M.L.C.C., 2012. Geomorfologia, estratigrafia de sequências e potencial de preservação dos Sistemas Laguna-Barreira do Quaternário costeiro do Rio Grande do Sul. Tese de doutoramento. Universidade Federal do Rio Grande do Sul, Porto Alegre.

Rosa, M.L.C.C., Barboza, E.G., Abreu, V.S., Tomazelli, L.J., Dillenburg, S.R., 2017. High-Frequency Sequences in the Quaternary of Pelotas Basin (coastal plain): A record of degradational stacking as a function of longer-Term base-level fall. Brazilian Journal of Geology. 47(2), 183–207. https://doi.org/10.1590/2317-4889201720160138.

Sánchez, L. E., Chaves, J. M., Franca Rocha, W. J., Lobão, J. S. B., & Martins Falcão, P., 2021. Identificação das Dunas do Atacama (Norte do Chile) a partir da avaliação de três algoritmos no Google Earth Engine. Revista Brasileira De Geografia Física, 14(6), 3294–3315. https://doi.org/10.26848/rbgf.v14.6.p3294-3315.

Sarmiento, G.N.R., Cipolletti, M.P., Perillo, M.M., Delrieux, C.A., Perillo, G.M.E., 2016. Methodology for classification of geographical features with remote sensing images: Application to tidal flats. Geomorphology. 257, 10-22. https://doi.org/10.1016/j.geomorph.2015.12.020.

Silva, C.G., Patchineelam, S.M., Baptista Neto, J.A. & Ponzi, V.R.A., 2004. Ambientes de Sedimentação Costeira e Processos Morfodinâmicos Atuantes na linha de Costa. In: Baptista Neto, J.A., Ponzi, V.R.A., Sichel, S.E. (Ed). Introdução à geologia marinha. Rio de janeiro, Interciência, p. 175-218.

Singh, S., Jagannadha Rao, M., Baranval, N. K., Kumar, K. V., Kumar, Y. V., 2023. Geoenvironment factors guided coastal urban growth prospect (UGP) delineation using heuristic and machine learning models. Ocean

& Coastal Management, v. 236, 1, 106496. https://doi.org/10.1016/j.ocecoaman.2023.106496.

Souza, M. C., Angulo, R. J., Assine, M. L., De Castro, D. L., 2012. Sequence of facies at a Holocene storm-dominated regressive barrier at Praia de Leste, southern Brazil. Marine Geology. 291–294, 49–62. https://doi.org/10.1016/j.margeo.2011.10.009.

Suguio, K., Martin, L., Bittencourt, A. C. S. P., Dominguez, J. M. L., Flexor, J.M., Azevedo, A. E. G., 1985. Flutuações do nível relativo do mar durante o quaternário superior ao longo do litoral brasileiro e suas implicações na sedimentação costeira. Revista Brasileira de Geociências. 15(4), 273–286.

Tomazelli, L.J., Villwock, J.A., 2000. O Cenozóico no Rio Grande do Sul: Geologia da Planície Costeira. In: Holz, M. & De Ros, L.F. (Eds.), Geologia do Rio Grande do Sul. Edições CIGO/UFRGS, Porto Alegre, 375-406.

Tomazelli, L. J., Villwock, J. A., 2005. Mapeamento Geológico de Planícies Costeiras: o Exemplo da Costa do Rio Grande do Sul. Gravel. 3, Porto Alegre – RS.

Vargas, R., Wasserman, J. C. de F. A., Silva, A. L. da, Tavares, T. L., Santos, C. A. dos, & Dias, F. F., 2021. Satellite-Derived Bathymetry Models from Sentinel-2A and 2B in the Coastal Clear Waters of Arraial do Cabo, Rio de Janeiro, Brazil. Revista Brasileira De Geografia Física, 14(5), 3078–3095. https://doi.org/10.26848/rbgf.v14.5.p3078-3095

Villwock, J.A., Tomazelli, L.J., Loss, E.L., Dehnhardt, E.A., Horn Filho, N.O., Bachi, F.A., Dehnhardt, B.A., 1986. Geology of the Rio Grande do Sul coastal province. In: Rabassa, J. (Eds.), Quaternary of South America and Antarctic Peninsula. Balkema, Rotterdam. 4,79-97.

Villwock, J. A., Tomazelli, L. J., 1995. Geologia costeira do Rio Grande do Sul. Centro de Estudos de Geologia Costeira e Oceânica. 8, 1–45.

Walsh, S.J., Butler, D.R., Malanson, G.P., 1998. An overview of scale, pattern, process relationships in geomorphology: a remote sensing and GIS perspective. Geomorphology. 21, 183-205.

Wang, L., Yang, Z., Sun, W., Fan, L., Tan, B., Zhou, Y., 2022. Processes of Tidal Flat Geomorphology Evolution Based on Time-Series Satellite Images. Remote Sens. 14, 4341. https://doi.org/10.3390/rs14174341.

Wu, W., 2007. Coastline evolution monitoring and estimation - a case study in the region of Nouakchott, Mauritania. International Journal of Remote Sensing, 28:24, 5461 — 5484. https://doi.org/10.1080/01431160701227612.

Yu, R.; Cai, H.; Zhang, B.; Feng, T., 2024. Multi-Scale Object Detection in Remote Sensing Images Based on Feature Interaction and Gaussian Distribution. Remote Sens.16, 1988. https://doi.org/10.3390/rs16111988.

Zangana, I., Otto, J.C., Mausbacher, R., Schrott, L., 2023. Efficient geomorphological mapping based on geographic information systems and remote sensing data: an example from Jena, Germany. Journal of Maps, vol. 19, 1, 2172468. https://doi.org/10.1080/17445647.2023.2172468.

Zhang, S., Ma, Y., Chen, F., Liu, J., Chen, F., Lu, S., Jiang, L., Li, D., 2020. A new method for supporting interpretation of paleochannels in a large scale — Detrended Digital Elevation Model Interpretation. Geomorphology. 369, 107374. https://doi.org/10.1016/j.geomorph.2020.107374.

Zhang, T., Cheng, C., Wu, X., 2023. Mapping the spatial heterogeneity of global land use and land cover from 2020 to 2100 at a 1 km resolution. Scientific Data[Online] 10. https://doi.org/10.1038/s41597-023-02637-7.